Spin-polarized electron momentum density distributions in $Pd_{1-x}Co_x$ alloys

J. W. Taylor,[1] J. A. Duffy,[1] J. Poulter,[2] A. M. Bebb,[1] M. J. Cooper,[1] J. E. McCarthy,[3] D. N. Timms,[4] J. B. Staunton,[1] F. Itoh,[5] H. Sakurai,[5] and B. L. Ahuja[6]

[1]*Department of Physics, The University of Warwick, Coventry, CV4 7AL, United Kingdom*

[2]*Department of Mathematics, Faculty of Science, Mahidol University, Rama 6 Road, Bangkok 10400, Thailand*

[3]*European Synchrotron Radiation Facility, BP 220, F-38043, Grenoble Cedex, France*

[4]*School of Earth and Environmental Science, The University of Portsmouth, Portsmouth, PO1 2DT, United Kingdom*

[5]*Department of Electronic Engineering, Gunma University, 1-5-1 Tenjin-Cho, Kiryu 376, Gunma, Japan*

[6]*Department of Physics, M. L. Sukhadia University, Udaipur-313001, India*

(Received 13 July 2001; revised manuscript received 12 October 2001; published 19 December 2001)

The spin-polarized momentum densities of disordered single-crystal $Pd_{1-x}Co_x$ have been studied using the magnetic Compton scattering technique, for the compositions $x=0.6$ and 0.28. Magnetic Compton profiles have been measured along the three principle crystallographic directions in each sample, and compared with theoretical profiles calculated using the Korringa-Kohn-Rostoker coherent-potential approximation method. The calculated and measured spin-polarized momentum distributions, as revealed by their magnetic Compton profiles, are in excellent agreement. However the calculated spin moment for the composition with $x=0.6$ is some 10% smaller than that measured experimentally, and for $x=0.28$, the deviation becomes 15%. These differences are attributed to the effect of order in the samples, which becomes increasingly important in the Pd-rich side of the phase diagram. The orbital component to the magnetization has been determined as 0.08 and $0.18\mu_B$ for $Pd_{0.4}Co_{0.6}$ and $Pd_{0.72}Co_{0.28}$, respectively.

DOI: 10.1103/PhysRevB.65.024442 PACS number(s): 75.50.Bb

I. INTRODUCTION

It is well known that alloys containing small concentrations of $3d$ ferromagnetic impurities such as Fe (Ref. 1) and Co in a Pd matrix dramatically alter the paramagnetic behavior of Pd, inducing ferromagnetism in the alloy. Crangle[2] and later Bozorth *et al.*[3] demonstrated that Pd becomes ferromagnetic when alloyed with $<1\%$ Fe or Co.

In this paper we report the use of magnetic Compton scattering (MCS) to determine the spin and orbital moments, and the spin-polarized electron momentum distributions (EMD) in ferromagnetic Pd-Co alloys. We are able to test the extent to which the self-consistent-field–Korringa-Kohn-Rostoker–Coherent-potential approximation (SCF-KKR-CPA) (Green's-function) method models these fundamental properties and show that the observed anisotropies in the EMD are associated with the low-momentum electrons in the minority-spin band.

Pd is a nearly ferromagnetic metal having a large Stoner enhancement of approximately 10. Dilute solid solutions of Co in Pd are often referred to as systems exhibiting giant magnetic moments due to the large polarizability of the Pd $4d$ bands of the host, by the $3d$ moments of the impurity ions. This has led to many investigations of the alloy system in the last three decades as the polarization of the electron cloud surrounding a Co atom in the dilute alloy regime is of the order of $7\mu_B$.[4]

More recently investigations of modulated layered structures of Pd and Co have renewed interest in the alloy system, as they exhibit large perpendicular anisotropy, a large magneto-optical Kerr effect,[5] and enhanced Co moments.[6] This has led to renewed theoretical efforts to model both the multilayered and the bulk alloy systems.[7,8]

Recent work has mainly centered on the magnetic x-ray circular dichroism (MXCD) technique,[6,11] which relies upon the validity of the sum rules[9] in order to extract values for the spin and orbital moments from the experimental dichroic signal. However, there is no simple relationship between the spin moment and the dichroism signal. Interpretation of the MXCD signal therefore relies upon theoretical assumptions of the sum rules in order that the spin and the orbital moments may be extracted from the dichroic absorption signal, unlike the MCS technique where the ground-state spin moment, and its spin-polarized momentum distribution, is deduced *empirically* from the experimental data. MXCD on Pd-Co multilayers[6] has shown that, in these systems, Co acquires an enhanced orbital moment of $0.25\mu_B$, which is twice that found in metallic Co.

Here we have investigated bulk alloys in the series $Pd_{1-x}Co_x$ ($x=0.4$ and 0.28), using magnetic Compton scattering to determine the spin-polarized momentum density distributions along the three main crystallographic directions. The experimental data are compared with KKR calculations in order to examine the effect of compositional order on both the spin moment in the alloy and the magnitude of the $3d$-$4d$ hybridization, as one goes from the Pd-rich to the Co-rich side of the phase diagram. The technique of magnetic Compton scattering is solely sensitive to the spin-polarized electrons and thus samples only the spin moment; after comparison with bulk magnetization measurements the orbital moment can be deduced, without the *necessity* of theoretical models. Furthermore the magnetic Compton profile is extremely sensitive to the various interband hybridizations that occur as a result of a local moment in a metallic matrix, since it samples the momentum contributions of all spin-polarized electrons from all bands. Thus the total spin moment is sampled directly. It is therefore an ideal technique for determining if the spin interaction is modeled correctly by theory.

The shape of the magnetic Compton profile intrinsically carries information about the overall localization of the moment, as the momentum-space wave function is related to the real-space wave function via a Fourier transform. The ability to comment upon the localization of the spin moment is a useful asset[12] when making comparisons with the theoretical magnetic Compton line shapes. The localization of the moment and its interaction with the surrounding conduction electrons, i.e., the *s*-*d* interaction, is the mechanism that drives the magnetism. The experimental spin-polarized momentum density profiles have been compared with those calculated using the Green's-function KKR approach. The quality of the agreement observed between theory and experiment is excellent; from the results, the induced Pd and Co moments are inferred, and by comparison with superconducting quantum interference device magnetization measurements the magnitude of the Co orbital component is also deduced.

Co forms a congruent solid solution with Pd across the entire range of compositions, with a chemically ordered phase existing at the composition Pd_3Co. Disordered single-crystal samples of $Pd_{40}Co_{60}$ and $Pd_{72}Co_{28}$ were produced using the Bridgman technique using starting elements of $4N$ purity. The samples for the magnetic Compton investigation were cut from the resulting boule in the form of thin discs of 8×0.1 mm. The samples were oriented in such a manner as to have the 100, 110, and 111 crystallographic directions in the plane of the disk, allowing the scattering vector to be aligned with each direction by an azimuthal sample rotation. The composition of each sample was checked using an energy dispersive x-ray technique, and the structure of the samples was verified using back reflection x-ray Laue photography.

II. MAGNETIC COMPTON SCATTERING

The Compton effect is observed when high-energy photons are inelastically scattered by electrons. The scattered-photon energy distribution is Doppler broadened, since the electrons have a finite momentum distribution. If the scattering event is described within the impulse approximation[10] the measured Compton spectrum is directly proportional to the scattering cross section.[13]

The Compton profile is defined as a one-dimensional (1D) projection onto the scattering vector of the electron momentum distribution $n(\mathbf{p})$, where the scattering vector is taken parallel to the z direction:

$$J(p_z)=\int\int n(\mathbf{p})dp_x dp_y . \tag{1}$$

The integral of $J(p_z)$ is the total number of electrons per unit cell.

MCS is a probe uniquely sensitive to the spin component of a material's magnetization. If the incident beam has a component of circular polarization, the scattering cross section contains a term that is spin dependent.[14] In order to isolate the spin dependence one must either flip the sample's direction of magnetization parallel and antiparallel with respect to the scattering vector or change the ''handedness'' of the photon helicity. Either method results in a magnetic Compton profile (MCP), $J_{\mathrm{mag}}(p_z)$, that is dependent upon only the unpaired spin in the sample, and is defined as the 1D projection of the spin-polarized electron momentum density:

$$J_{\mathrm{nag}}(p_z)=\int\int [n^{\uparrow}(\mathbf{p})-n^{\downarrow}(\mathbf{p})]dp_x dp_y . \tag{2}$$

Here $n^{\uparrow}(\mathbf{p})$ and $n^{\downarrow}(\mathbf{p})$ are the momentum densities of the majority- and minority-spin bands. The integral of the MCP is the total spin moment per formula unit (F.U.) in the sample. MCS is an established technique for determining spin-polarized electron densities.[15–17] Within the impulse approximation the method is insensitive to the orbital moment.[18] Unlike MXCD MCS samples all the spin-polarized electrons regardless of their binding energies and wave-function symmetries.

III. EXPERIMENT AND DATA ANALYSIS

The magnetic Compton profiles of $Pd_{0.4}Co_{0.6}$ and $Pd_{0.72}Co_{0.28}$ resolved along the three major crystallographic directions were measured at the high-energy beamline ID15A at the European Synchrotron Radiation Facility (ESRF), France. The experiment was performed in transmission geometry at $T=300\pm1$ K. An incident-beam energy of 200 keV was selected using a Si 311 monochromator in Laue geometry. At these photon energies, which are desirable for optimum resolution and interpretation within the impulse approximation, reversing the helicity of the incident photons is not yet practical. The spin-dependent signal was isolated by reversing the sample's magnetization vector using a 1-T rotating permanent magnet. Circular polarization was produced by selecting a beam approximately 2 μrad below the orbital plane of the synchrotron,[19] this value being chosen to maximize the ratio of magnetic scattering to statistical noise in the charge scattering. A degree of circular polarization of about 45% was obtained. The energy spectrum of the scattered flux was measured using a Ge detector at a mean scattering angle of 170°. The momentum resolution of the magnetic Compton spectrometer, taken as the full width at half maximum (FWHM) of the instrument response function, was 0.40 a.u. (where 1 a.u. $=1.99\times10^{-24}$ kg m s^{-1}).

The total number of counts in the charge Compton profiles was 2×10^8, corresponding to a statistical precision of $\pm2\%$ in the resulting MCP, in a bin width of 0.1 a.u. Since the MCP is the difference between two charge Compton profiles, components arising from spin-paired electrons and from most sources of systematic error are effectively canceled out. The data were corrected for energy-dependent detector efficiency, sample absorption, and the relativistic scattering cross section. The magnitude of the magnetic multiple scattering was determined to be no more than 0.012%. The profiles were corrected for multiple scattering using the technique described by Felsteiner, Pattison, and Cooper.[20] After checking that the resulting spectra were symmetric about $p_z=0$, the profiles were folded to improve the effective statistics. The profile areas were normalized to an absolute spin moment scale using Fe data taken under the same conditions.

IV. CALCULATION OF $J_{mag}(P_z)$ USING THE SCF-KKR-CPA METHOD

The spin-dependent momentum densities of $Pd_{0.4}Co_{0.6}$ and $Pd_{72}Co_{28}$ were calculated using the KKR Green's-function method[21–23] within the CPA (Refs. 24–26) and the atomic sphere approximation.[27] Our approach has been to calculate the momentum density $n(\mathbf{p})$ and integrate directly around a contour in the complex energy plane. The isotropic potentials are placed onto a crystal lattice structure, which in turn invokes directional anisotropies in the calculated wave functions. The exchange-correlation component of the potential was described in the local spin-density approximation (LSDA).[28] The method is described more fully elsewhere.[29] The momentum density is given, in terms of the Green's function $G(\mathbf{p},z)$, by

$$n(\mathbf{p}) = -\int \frac{dE}{\pi} f(E)\,\mathrm{Im}\,G((\mathbf{p});E+i\eta), \tag{3}$$

where $n(\mathbf{p})$ is expressed as an integral over real E above the axis by η. $f(E)$ denotes the Fermi factor (since our calculations are done at finite temperature).

Double integration of the momentum density $n(\mathbf{p})$ along the crystallographic direction results in the determination of the charge Compton profile $J(p_z)$. The solid solution of Co in Pd was simulated using a disordered arrangement of atoms on an fcc lattice with the experimentally determined lattice spacing of 7.00 and 7.22 a.u. for $Pd_{0.4}Co_{0.6}$ and $Pd_{72}Co_{28}$, respectively. The averaging over the disorder is done adequately by the coherent-potential approximation. The calculations were performed on a grid of 65 points on the complex energy contour. The directional charge Compton profiles (including contributions from the core and the valence electrons) behaved as expected in the large momentum region of the profile showing a free-atom-like monotonic decrease to zero. A similar calculation was performed for pure Co on the same fcc lattice for comparison.

In this regime the Co spin moment was determined to be 1.77 and $2.01\mu_B$ per atom for $Pd_{0.4}Co_{0.6}$ and $Pd_{72}Co_{28}$, respectively. The induced spin moment on the Pd site was determined as $\approx 0.21\mu_B$ per atom for both samples. This yields a total spin moment of $1.15\mu_B$ per formula unit for $Pd_{0.4}Co_{0.6}$ and $0.71\mu_B$ for $Pd_{0.72}Co_{0.28}$, which are in reasonable agreement with those measured previously.[32,8] The resulting theoretical charge Compton profiles were convoluted with a Gaussian of FWHM 0.4 a.u. to simulate the experimental resolution function and thus allow a direct comparison with experiment. The theoretical MCP's were then produced by taking the difference of the resolution-broadened spin-up and -down charge Compton profiles.

V. RESULTS AND DISCUSSION

A. $Pd_{0.4}Co_{0.6}$

The experimental spin-polarized Compton profiles for $Pd_{40}Co_{60}$ are compared with the calculated profiles in Figs. 1–3 for the crystallographic directions 100, 110, and 111, respectively. The experimentally determined spin moment for this composition given by the integrated area of the MCP

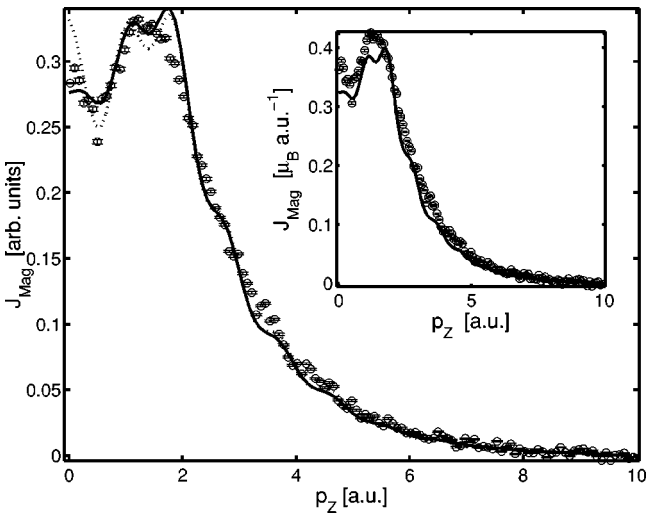

FIG. 1. The experimental MCP (circles) and calculated KKR MCP (full line) for $Pd_{0.4}Co_{0.6}$ resolved along the 100 crystallographic direction. The dotted line indicates the calculated magnetic profile for pure Co on an fcc lattice (data are normalized to have equal areas to facilitate comparison). The inset shows the experimental (circles) and calculated (full line) KKR data normalized to the experimental and calculated spin moments.

[Eq. (2)] was $1.28\pm0.02\mu_B$ per formula unit (see Table I), which is in reasonable agreement with that calculated. The KKR calculated spin moment is underestimated at this composition by ≈8%. This discrepancy between the theoretical and experimental spin moments is illustrated in the insets to Figs. 1–3, for the three crystallographic directions measured, where each profile is normalized to the experimental and calculated spin moments.

The total moment measured using an Oxford Instruments 12-T vibrating sample magnetometer was determined as $1.330\pm0.001\mu_B$ per formula unit. Assuming that there is negligible orbital contribution to the induced Pd moment the

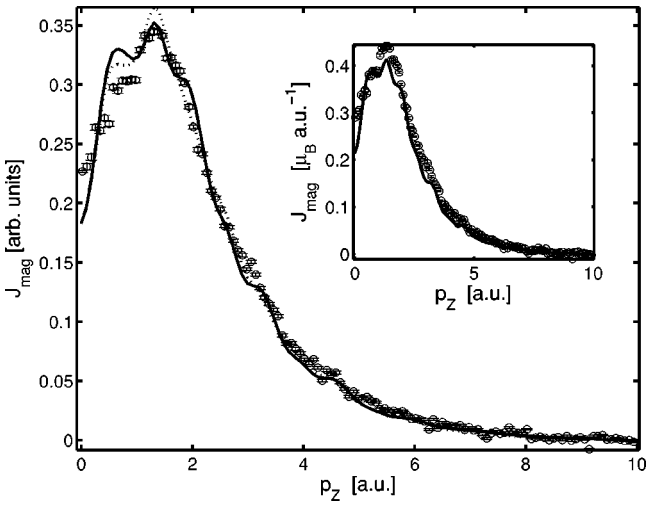

FIG. 2. The experimental MCP (circles) and calculated KKR MCP (full line) for $Pd_{0.4}Co_{0.6}$ resolved along the 110 crystallographic direction. Details for the main figure and the inset are identical to those stated for Fig. 1.

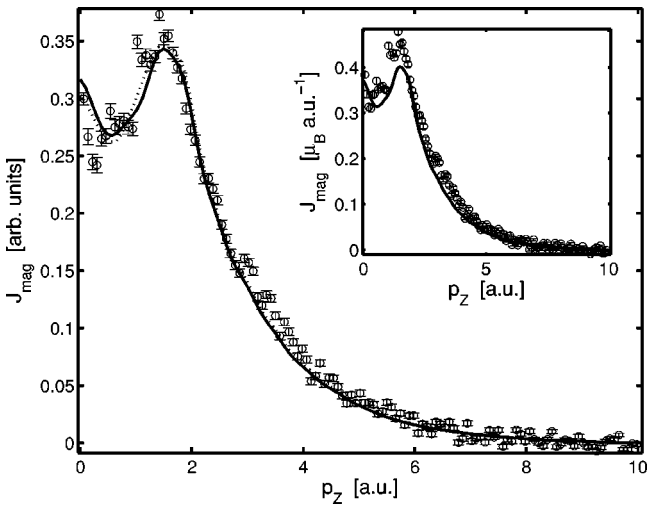

FIG. 3. The experimental MCP (circles) and calculated KKR MCP (full line) for $Pd_{0.4}Co_{0.6}$ resolved along the 111 crystallographic direction. Details for the main figure and the inset are identical to those stated for Fig. 1.

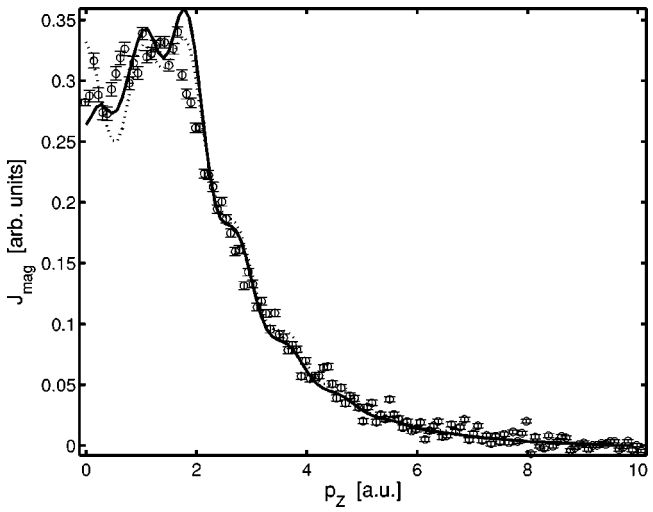

FIG. 4. The experimental MCP (circles) and calculated KKR MCP (full line) for $Pd_{0.72}Co_{0.28}$ resolved along the 100 crystallographic direction. The dotted line indicates the calculated magnetic profile for pure Co on an fcc lattice (data are normalized to have equal areas).

orbital contribution per Co atom is then $0.08 \pm 0.02\ \mu_B$. This value is in reasonable agreement with those calculated by Eriksson *et al.*[30] who quoted an orbital moment in metallic fcc Co as $0.12\ \mu_B$ using the linear muffin-tin orbital (LMTO) method with spin-orbit coupling and $0.07\ \mu_B$ with no spin-orbit coupling, and also those of Igarashi and Hirai[31] who used a tight-binding scheme with and without enhancement to calculate the orbital moment of fcc Co as 0.085 and $0.135\ \mu_B$, respectively.

If the experimental and calculated profiles are renormalized to have the same area, i.e., the same moment, excellent agreement between the line shape of the experimental and calculated profiles is observed for all three directions. Umklapp features in the experimental profile are correctly modeled by the calculation as is the region at low momentum. The dotted lines in Fig. 1–3 show the magnetic Compton profile calculated for fcc Co; it is clear that the calculation for the alloy $Pd_{0.4}Co_{0.6}$ gives far better agreement of the Compton profile line shape in the region 0–2 a.u. for the 100 direction as compared to the fcc Co MCP, whereas in the 110 and 111 directions the improvement is less dramatic. An induced moment on a $4d$ band, as is thought to occur in these alloys, will have a similar spin-polarized momentum distribution to that of a $3d$ band, in that the spin-polarized momentum distribution will persist to ≈ 6 a.u. It is therefore difficult to separate quantitatively the contribution from the $4d$ Pd moment and that from the Co $3d$ moment. In the case of $Pd_{0.4}Co_{0.6}$ there appears to be only a slight difference between the experimental profile and that of the calculated fcc Co in this region, implying that any $4d$ Pd moment is very small. The conduction-electron polarization component to the magnetism (which is important in the region of <2 a.u.) appears to have a significant directional dependence (see Sec. V C).

TABLE I. Experimental and calculated spin and derived orbital moments for $Pd_{0.4}Co_{0.6}$ and $Pd_{0.72}Co_{0.28}$.

	$Pd_{0.4}Co_{0.6}$	$Pd_{0.72}Co_{0.28}$
MCS spin moment [μ_B f.u.$^{-1}$]	1.28(2)	0.85(5)
KKR spin moment [μ_B f.u.$^{-1}$]	1.15	0.71
Total moment [μ_B f.u.$^{-1}$]	1.33	0.9
$\mathbf{M}_L$ [μ_B Co^{-1}]	0.08(2)	0.18(5)

B. $Pd_{0.72}Co_{0.28}$

The experimental spin-polarized Compton profiles for $Pd_{72}Co_{28}$ are compared with the calculated profiles in Figs. 4–6 for the crystallographic directions 100, 110, and 111, respectively. The experimentally determined spin moment for this composition was $0.85 \pm 0.05\ \mu_B$ per formula unit, see Table I, which is in good agreement with that determined previously.[32] This yields an orbital contribution per Co atom of $0.18 \pm 0.05\ \mu_B$, which is again in good agreement with that quoted by Miyahaza *et al.*[11] The calculation underestimates the spin moment by $\approx 15\%$.

Again, when the profiles are renormalized to the same area (i.e., spin moment) excellent agreement between calculated and measured line shapes is observed and Umklapp features coincide in the calculated profile and the experimental MCP. If one compares the calculated profiles for $Pd_{0.72}Co_{0.28}$ and fcc Co, a larger deviation is observed at higher momenta, as one may expect if a $4d$-type moment is induced on the Pd. Again in the 100 direction the calculated profile for $Pd_{0.72}Co_{0.28}$ yields an improved fit over that predicted for pure fcc Co in the low-momentum region of the MCP. Conversely the low-momentum spin distribution along the 111 direction for $Pd_{0.72}Co_{0.28}$ appears to be wholely Co in character.

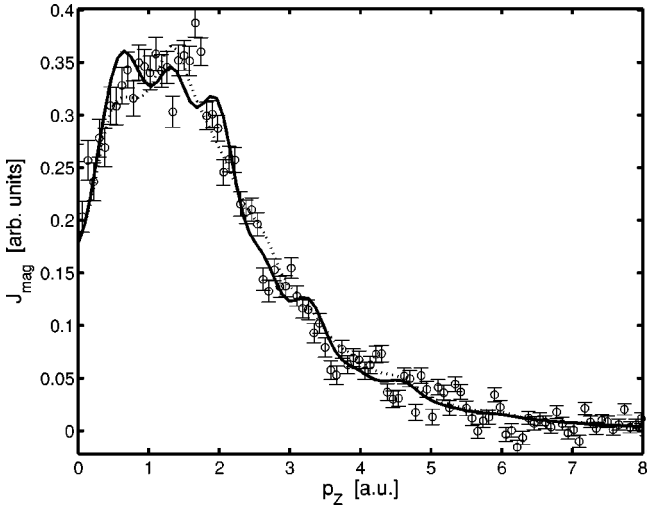

FIG. 5. The experimental MCP (circles) and calculated KKR MCP (full line) for $Pd_{0.72}Co_{0.28}$ resolved along the 110 crystallographic direction. The dotted line indicates the calculated magnetic profile for pure Co on an fcc lattice (data are normalized to have equal areas).

C. Majority- and minority-spin bands for $Pd_{0.4}Co_{0.6}$

From the directional magnetic Compton profiles the majority- and the minority-spin band momentum density distributions may be calculated, thus:

$$J(\uparrow)_{\mathrm{maj}} = \tfrac{1}{2}[J(p_z)_{\mathrm{charge}} + J(\dot{p}_z)_{\mathrm{spin}}], \tag{4}$$

$$J(\downarrow)_{\mathrm{min}} = \tfrac{1}{2}[J(p_z)_{\mathrm{charge}} - J(p_z)_{\mathrm{spin}}], \tag{5}$$

where $J_{\mathrm{charge}}(p_z)$ and $J_{\mathrm{spin}}(p_z)$ are the charge and magnetic Compton profiles, respectively. Here the majority and minority bands are dominated by contributions from the core levels. In order to separate the spin-polarized majority- and minority-spin band contributions from those of the core-level components the difference between two crystallographic directions is evaluated, resulting in the determination of the directional dependence of the majority- and minority-spin band momentum densities:

$$\Delta J(\uparrow)_{111\text{-}100} = [J(\uparrow)_{\mathrm{maj}111} - J(\uparrow)_{\mathrm{maj}100}]. \tag{6}$$

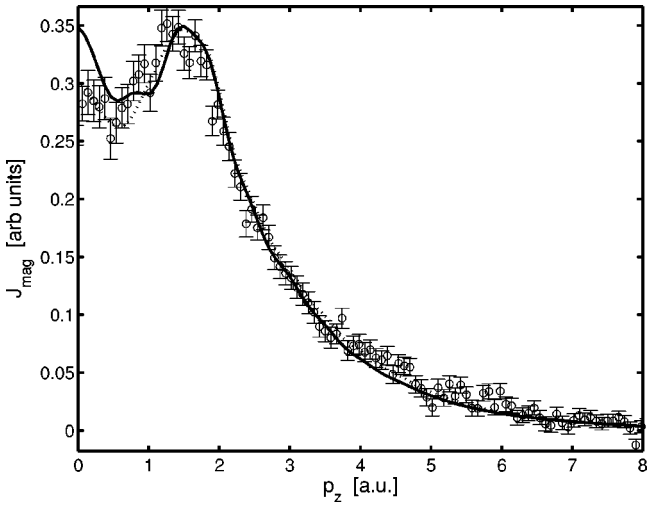

FIG. 6. The experimental MCP (circles) and calculated KKR MCP (full line) for $Pd_{0.72}Co_{0.28}$ resolved along the 111 crystallographic direction. The dotted line indicates the calculated magnetic profile for pure Co on an fcc lattice (data are normalized to have equal areas).

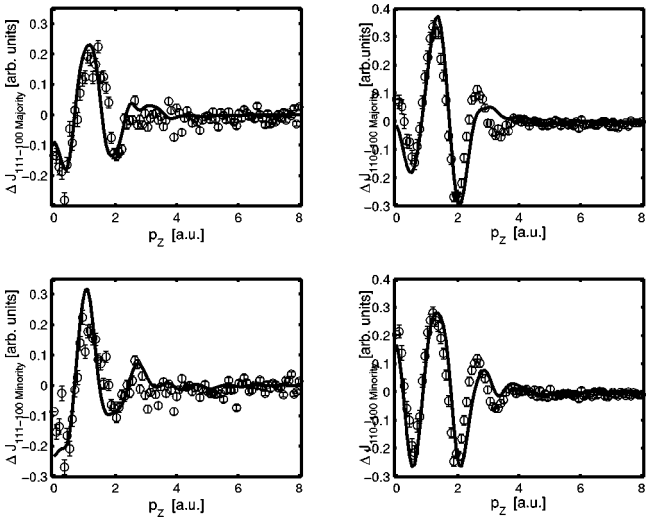

FIG. 7. The majority- (upper plots) and minority- (lower plots) spin band Compton profile anisotropies calculated for the 111-100 and 110-100 directions (circles) compared with the resolution-corrected (0.4 a.u.) calculated KKR anisotropies (full line).

The majority- and the minority-spin band momentum density anisotropic distributions for $Pd_{0.4}Co_{0.6}$ have been evaluated for the 111-100 and the 110-100 crystallographic directions, compared with the resolution-corrected distributions calculated from the KKR spin-polarized momentum densities, and presented in Fig. 7. The agreement is again excellent, showing that the KKR method correctly models the aspherical component of the spin density. It is clear from Fig. 7 that above $\approx$0.5 a.u., the directional differences in the majority and minority bands are similar in periodicity and amplitude; at higher momenta the distributions are effectively isotropic. Differences appear at very low momenta ($p_z < 0.5$ a.u.), where it is clear that the greater anisotropy is associated with the minority band electrons.

This is evidence that the anisotropic contribution to the magnetism in PdCo alloys is influenced by the minority band electrons. Comparing the directional profiles in Figs. 1–3, there is a large degree of anisotropy in the low ($p_z < 0.5$ a.u.) region. From the directional spin band anisotropies it is tempting to infer that the anisotropic distribution occurs mainly due to contributions from the minority-spin band components of the magnetization.

VI. DISCUSSION

The fact that the calculated and measured magnetic Compton line shapes give such good agreement, whereas the overall spin moments show a discrepancy, at first seems anomalous. However there are several points at which the

model may not fully represent the actual material. These are the failure of the theoretical model to determine correctly the exchange splitting, i.e., inclusion of the CPA in the calculation to average over the disorder in the model, and the fact that the calculation assumes total disorder of the solid solution of Co in Pd whereas our sample had a finite degree of order. Further one must consider that although the LSDA works well for elemental ferromagnets in the $3d$ series it may not be perfect when applied to a disordered binary alloy. These differences will now be discussed more fully.

In the $Pd_{1-x}Co_x$ system, the nearest-neighbor interaction between Co and Pd is a critical factor for the induced moment on the Pd site.[8] The calculation assumes complete disorder across the fcc lattice and this is of course not the case in our samples, where the structural order parameter has been determined as 0.5 and 0.2 for $Pd_{0.72}Co_{0.28}$ and $Pd_{0.4}Co_{0.6}$, respectively. The number of nearest-neighbor Co-Pd interactions is reduced from four to three as one moves from the ordered to the disordered regime, thus the induced moment of Pd is reduced. The induced Pd moment has been calculated as $0.38\,\mu_B$ in the ordered phase of Pd_3Co and $0.24\,\mu_B$ in the case of the disordered alloy. Thus the overall spin moment is 0.82 for Pd_3Co and $0.725\,\mu_B$ f.u.$^{-1}$ for $Pd_{0.75}Co_{0.25}$. Applying the values for the ordered system to our sample and assuming that our sample has a characteristic local environment similar to Pd_3Co then, the calculated spin moment becomes $0.87\,\mu_B$ f.u.$^{-1}$, which is closer to the experimental value. The orbital moments deduced for $Pd_{0.4}Co_{0.6}$ and $Pd_{0.72}Co_{0.28}$ in Table I differ by a factor of ≈ 2. This difference is attributed to the effect of compositional order, i.e., the number of nearest-neighbor interactions on the crystalline electric field and the spin-orbit coupling factor. The values we calculate are in good agreement with those measured and calculated previously by a number of different methods.

When the difference between the experimental and calculated spin-polarized momentum densities are closely examined (see the insets to Figs. 1–3), it is apparent that there are simply not enough spin-polarized electrons in the calculated profiles. The agreement between the calculated and measured spin moments is good for both the compositions measured. The fact that the theoretical model does not accurately calculate the spin moment, yet correctly calculates the momentum density distribution, has been observed before[33] in band-structure calculations for Ni and in KKR-type calculations[34] for Fe_3Si. The differences between the calculated and measured spin moments in our case are similar to those found by Dixon *et al.*[33] in Ni, which indicates that the LSDA is a reasonable approximation in the case for this binary $3d$ alloy. The reasons for the theoretical discrepancy may be the variation of lattice spacing between that measured experimentally and that calculated; also one must consider the inclusion of the CPA to deal with the disorder in this system, which will effect the calculated spin moment.

Despite this, the KKR model predicts correctly the localization of the spin moment. This is in contrast with the case for Fe, where LMTO and full potential augmented plane-wave models incorrectly derive the d-band localization and thus fail to model correctly the low-momentum components to the magnetic Compton profile.[12] A similar systematic deviation is observed in the case of $Pd_{0.72}Co_{0.28}$, but here the deviation is slightly larger. We attribute these discrepancies to the effects of order in the samples since the Pd induced moment is critically dependent upon this parameter. It is clear then that the spin moment in the PdCo alloy series is strongly influenced by disorder in the sample. Previous interpretation of the PdCo alloy series in the dilute limit using the KKR method has assumed that Co sites represent a local-moment impurity, producing a spin polarization in neighboring Pd sites. Summation of the induced Pd polarization across a number of coordination spheres results in an enhanced moment in the cluster. The spin-polarized density of states[4] resulting from the aforementioned model implies that impurity spin-down d bands are strongly hybridized with the host spin-down d-band electrons. This hybridization is assumed to occur over the whole d band. The magnetic Compton profiles for $Pd_{0.72}Co_{0.28}$ when compared with the KKR Compton profiles for the alloy and fcc Co clearly show that the effect of introducing Co into the Pd host matrix is a broad hybridization of the Co $3d$ with the Pd $4d$ band. This is clear evidence that the single-site impurity approach is valid for this system.

VII. SUMMARY

From our results it is clear that the KKR method of calculating spin-polarized momentum density distributions in the PdCo system gives good results; we have attributed deviations of the calculated spin moment to the effect of order in our experimental samples. From this it is clear that the alloy system is strongly dependent on the order parameter. The good agreement between the line shapes of the calculated and experimental magnetic Compton profiles demonstrates that the $4d$-$3d$-band hybridization is modeled well by the KKR calculation and that, within our experimental resolution function (0.4 a.u.), the magnetic Compton profile is insensitive to compositional order. The good agreement of the low-momentum components of the magnetic Compton profiles, and the directional anisotropies, illustrate that the s-d interaction in the alloy system is also well modeled.

ACKNOWLEDGMENTS

The authors wish to thank the EPSRC United Kingdom for funding this work, the ESRF for provision of beam time, V. Honkimaki and T. Buslaps of the high-energy beamline for their help, and M. Lees for performing magnetization measurements. One of the authors, J.P., wishes to thank the Thailand Research Fund, Contract No. RTA/02/2542 for funding, and the High Performance Computing Center, NECTEC, Thailand, for computational facilities. The authors are grateful to D. D. Johnson for the provision of self-consistent KKR-CPA potentials for the two Pd-Co alloys.

[1] F. W. Constant, Phys. Rev. **36**, 1654 (1930).
[2] J. Crangle, Philos. Mag. **5**, 335 (1960).
[3] R. M. Bozorth, P. A. Wolff, D. D. Davis, V. B. Compton, and J. H. Wernick, Phys. Rev. **122**, 1157 (1961).
[4] A. Oswald, R. Keller, and P. H. Dederichs, Phys. Rev. Lett. **56**, 1419 (1986).
[5] D. G. Stinson and S. C. Shin, J. Appl. Phys. **67**, 317 (1990).
[6] Y. Wu, J. Stohr, B. D. Hermsmeier, M. G. Samant, and D. Weller, Phys. Rev. Lett. **69**, 2307 (1992).
[7] A. Jezierski, J. Magn. Magn. Mater. **123**, L1 (1993).
[8] S. Kaprzyk, A. Z. Maksymowicz, and K. Zakrzewska, J. Magn. Magn. Mater. **104-107**, 2019 (1992).
[9] B. T. Thole, Paolo Carra, F. Sette, and G. van der Laan, Phys. Rev. Lett. **68**, 1943 (1992).
[10] P. M. Platzman and N. Tzoar, Phys. Rev. B **2**, 3556 (1970).
[11] T. Miyahara, S. Y. Park, T. Hanyu, T. Hatano, S. Moto, and Y. Kagoshima, Rev. Sci. Instrum. **66**, 1558 (1995).
[12] J. W. Taylor, J. A. Duffy, A. M. Bebb, M. J. Cooper, S. B. Dugdale, J. E. McCarthy, D. N. Timms, D. Greig, and Y. B. Xu, Phys. Rev. B **63**, R220404 (2001).
[13] P. Holm, Phys. Rev. A **37**, 3706 (1988).
[14] F. Bell, J. Felsteiner, and L. P. Pitaevskii, Phys. Rev. A **53**, R1213 (1996).
[15] J. A. Duffy, S. B. Dugdale, J. E. McCarthy, M. A. Alam, M. J. Cooper, S. B. Palmer, and T. Jarlborg, Phys. Rev. B **61**, 14 331 (2000).
[16] J. E. McCarthy, J. A. Duffy, C. Detlefs, M. J. Cooper, and P. C. Canfield, Phys. Rev. B **62**, R6073 (2000).
[17] J. A. Duffy, J. E. McCarthy, S. B. Dugdale, V. Honkimaki, M. J. Cooper, M. A. Alam, T. Jarlborg, and S. B. Palmer, J. Phys.: Condens. Matter **10**, 10 391 (1998).
[18] P. Carra, M. Fabrizio, G. Santoro, and B. T. Thole, Phys. Rev. B **53**, R5994 (1996).
[19] J. E. McCarthy, M. J. Cooper, P. K. Lawson, D. N. Timms, S. O. Manninen, K. Hamalainen, and P. Suortti, J. Synchrotron Radiat. **4**, 102 (1997).
[20] J. Felsteiner, P. Pattison, and M. J. Cooper, Philos. Mag. **30**, 537 (1974).
[21] J. Korringa, Physica (Amsterdam) **13**, 392 (1947).
[22] W. Kohn and N. Rostoker, Phys. Rev. **94**, 1111 (1954).
[23] J. S. Faulkner, J. Phys. C **10**, 4661 (1977).
[24] P. Soven, Phys. Rev. **156**, 809 (1967).
[25] G. M. Stocks, W. M. Temmerman, and B. L. Gyorffy, Phys. Rev. Lett. **41**, 339 (1978).
[26] D. D. Johnson, D. M. Nicholson, F. J. Pinski, B. L. Gyorffy, and G. M. Stocks, Phys. Rev. B **41**, 9701 (1990).
[27] O. K. Andersen, Phys. Rev. B **12**, 3060 (1975).
[28] O. Gunnarsson and B. I. Lunqvist, Phys. Rev. B **13**, 4274 (1976).
[29] J. Poulter and J. B. Staunton, J. Phys. F: Met. Phys. **18**, 1877 (1988).
[30] O. Eriksson, B. Johansson, R. C. Albers, A. M. Boring, and M. S. S. Brooks, Phys. Rev. B **42**, R2707 (1990).
[31] J. Igarashi and K. Hirai, Phys. Rev. B **53**, 6442 (1996).
[32] J. W. Cable, E. O. Wollan, and W. C. Koehler, Phys. Rev. A **138**, A755 (1965).
[33] M. A. Dixon, J. A. Duffy, S. Gardelis, J. E. McCarthy, M. J. Cooper, S. B. Dugdale, T. Jarlborg, and D. N. Timms, J. Phys.: Condens. Matter **10**, 2759 (1998).
[34] E. Zukowski, A. Andrejczuk, L. Dobrzynski, S. Kaprzyk, M. J. Cooper, J. A. Duffy, and D. N. Timms, J. Phys.: Condens. Matter **12**, 7229 (2000).